Original communication

MRI detects increased aortic stiffening and myocardial dysfunction after TEVAR of blunt injury in young patients

Tamer Ghazy[1,a] , Bettina Kirstein[2,a] , Jakub Tomala[3] , Igli Kalaja[4] , Jörg Herold[5], Marc Irqsusi[1] , Ardawan Rastan[1] , Helmut Karl Lackner[6] , Norbert Weiss[7], and Adrian Mahlmann[7,8]

[1] Department of Cardiac and Thoracic Vascular Surgery, Marburg University Hospital, Germany

[2] Department of Rhythmology, University Heart Center Lübeck, University Hospital Schleswig-Holstein, Germany

[3] Department of Electrophysiology, Heart Center, Technische Universität Dresden, Germany

[4] Center of Cardiology, Cardiology III – Angiology, University Medical Center of the Johannes Gutenberg University, Mainz, Germany

[5] Department of Vascular Medicine – Angiology, Klinikum Darmstadt GmbH, Germany

[6] Division of Physiology, Otto Loewi Research Center for Vascular Biology, Immunology and Inflammation, Medical University of Graz, Austria

[7] Department of Internal Medicine III, University Hospital Carl Gustav Carus, Technische Universität Dresden, Germany

[8] Center for Vascular Medicine, Clinic of Angiology, St.-Josefs-Hospital, Katholische Krankenhaus Hagen gem. GmbH, Germany

[a] The authors share the first authorship.

Summary: *Background:* Thoracic endovascular aortic repair (TEVAR) is a well-established technique for the management of blunt thoracic aortic injury (BTAI). Despite improvements in vascular imaging, graft material properties, and implant techniques, stent-graft deployment artificially induces aortic stiffening. This study aimed to evaluate the midterm effect of thoracic endovascular aortic repair after blunt thoracic aortic injury on aortic stiffness and cardiac function in young patients using cardiovascular magnetic resonance (CMR) imaging. *Patients and methods:* From all patients who underwent TEVAR for BTAI between 2009 and 2019 in a single institution, 10 patients with no other comorbidities affecting arterial stiffness were sex-, age-, height-, and body surface area-matched to 10 healthy controls. Comprehensive CMR examination was performed in all controls and patients. The mean follow-up period was 5.4±1.8 years; the mean age at the time of TEVAR was 30.3±8.7 years. *Results:* Four patients who underwent TEVAR developed arterial hypertension. 4D flow CMR-based analysis demonstrated higher global pulse wave velocity (PWV) in TEVAR patients than in controls (p=0.012). Segmental analysis showed a higher PWV in the descending and abdominal aorta. The indexed diameter of the ascending aorta was larger in TEVAR patients than in controls (p=0.007). The CINE acquisitions demonstrated increased left ventricular myocardial thickness (p<0.001). The 3D global diastolic strain rate and diastolic longitudinal velocity (e′) decreased, and the A-wave velocity increased. Native myocardial T1 values were significantly higher in TEVAR patients (p=0.037). *Conclusions:* Young patients with TEVAR after BTAI are at an increased risk of developing vascular and myocardial dysfunction due to increased aortic stiffness. CMR follow-up allows for a comprehensive and radiation-free evaluation of vascular stiffness and associated myocardial changes, especially at the early and subclinical stages.

Keywords: Aortic stiffness, diastolic function, 4D flow, magnetic resonance imaging, blunt thoracic aortic injury, thoracic endovascular aortic repair

Introduction

Thoracic endovascular aortic repair (TEVAR) is a well-established technique for the management of blunt thoracic aortic injury (BTAI) [1, 2]. Despite improvements in vascular imaging, graft material properties, and implant techniques, stent-graft implantation artificially induces aortic stiffening [3]. As many patients who undergo TEVAR for BTAI are young, the long-term effects of this increased aortic stiffening may have an effect on these patients'

Table I. Baseline demographics

Variable	TEVAR group (N=10)	Healthy control group (N=10)	p-value
Age (years) at follow-up	37; 30.0–41.8	36; 29.8–41.5	0.980
Age (years) at the time of TEVAR	29; 25.3–37.530±8.7		
Gender (female)	N=2	N=2	
Height (cm)	173.5; 170.5–185.5	178.5; 170.3–184.3	0.893
Body weight (kg)	75.0; 68.5–87.3	74.5; 69–89.5	0.964
Body surface area (m^2)	1.9; 1.8–2.0	1.9; 1.8–2.1	0.990

Notes. TEVAR: thoracic endovascular aortic repair; N: number of patients. Metrics as median and interquartile range.

morbidity over time. There is only a limited amount of data available regarding the analysis of these effects, and even fewer data studying their different diagnostic tools.

The aim of this study was to gain a better understanding of the aortic and cardiac morphological and hemodynamic changes after TEVAR, especially in young patients with aortic injury by traumatic cause, without cardiovascular risk factors or atherosclerotic manifestations. So far, oscillometric methods have been used for measuring vascular stiffness by pulse wave velocity. In this study, we evaluated the effect of TEVAR after BTAI on aortic stiffness and cardiac function using the innovative non-contrast magnetic resonance imaging as a 4-dimensional strategy.

Patients and methods

Ethical approval

This study was performed in compliance with the Declaration of Helsinki and approved by the ethics committee of the Medical Faculty of Technische Universität Dresden (approval numbers: EK 317082014 for patients and EK 186042019 for healthy controls). Written informed consent was obtained from all patients and healthy controls.

Patient enrolment

Between November 2009 and November 2019, 653 patients with polytrauma who were admitted to the emergency department of a tertiary institution were retrospectively screened for study inclusion. Data were collected from an electronic database at the Dresden University Hospital of the Dresden University of Technology, Germany, which included all admitted patients. The inclusion criteria were patients aged >18 years up to a maximum age of 50 years with polytrauma as a cause of admission and who were diagnosed with aortic rupture as a blunt thoracic aortic injury (BTAI) in the descending thoracic aorta, and treated by thoracic endovascular aortic repair (TEVAR) with the stent-graft located in zone 2 (according to the classification proposed by Ishimaru [4]). Patients with relevant cardiovascular risk factors (past or current smoking status, diabetes mellitus, arterial hypertension before treatment with TEVAR, and hypercholesterolemia), comorbidities (atherosclerotic or inflammatory cardiovascular disease

and known connective tissue disease) with a potential impact on arterial stiffness, and prior aortic surgical or endovascular interventions or contraindications for magnetic resonance imaging (MRI) were excluded. Fourteen patients met these criteria. Ten of the 14 identified patients gave consent to participate in the study and were included. Detailed demographics and clinical characteristics of the study cohort and clinical data of the TEVAR procedures are shown in Tables I and II, respectively.

Recruitment of matched healthy controls

Patients in the TEVAR group were matched with healthy controls. First, matching candidates were screened, and candidates with preexisting cardiovascular risk factors (past or current smoking status, diabetes mellitus, arterial hypertension, and hypercholesterolemia), already known and documented comorbidities (atherosclerotic or inflammatory cardiovascular disease and connective tissue disease), and prior aortic surgical or endovascular interventions were excluded. The remaining candidates were defined as healthy and were screened for matching with the TEVAR group. The matching criteria were sex, age (maximum age difference, 5 years), height (maximum difference, 10 cm), and body mass index (maximum difference, 10 kg; Table I). A total of 10 patients were included in the control group.

Study measurements

Owing to the post-hoc cross-sectional design of the study, examination of pulse wave velocity and strain by MRI were performed once at the latest presentation for follow-up after TEVAR.

Echocardiography and clinical outcomes

Echocardiography was performed to assess the left ventricular systolic and diastolic functions and to evaluate hypertrophy (Philips iU22 Ultrasound Machine, Philips Ultrasound Inc., Reedsville, PA, USA). The collected parameters included the left ventricular diameters (left ventricular end-systolic and end-diastolic diameters), ejection fraction (%), and the wall thickness of the interventricular septum and posterior left ventricular wall (mm) to exclude asymmetric hypertrophy. The diastolic function

Table II. Detailed procedures and results in TEVAR group

No.	Age (years) at the time of TEVAR	Gender (m/f)	Trauma	Diagnosis	Stent type	Stent measurements proximal/distal/length (mm)
1	43	m	CA	TAR	Gore TAG	31/31/150
2	40	m	MCA	TAR	Gore TAG	26/26/100 and 28/28/150
3	26	m	CA	TAR	Medtronic Valiant	24/24/150
4	19	m	MCA	TAR	Gore TAG	28/28/100 and 31/31/100
5	38	f	CA	TAR	Gore TAG	28/28/150
6	36	m	CA	TAR	Gore TAG	26/26/100
7	25	m	MCA	TAR	Gore TAG	22/22/150
8	27	m	MCA	TAR	Gore TAG	26/26/100
9	31	m	CA	TAR	Gore TAG	21/21/100
10	18	f	CA	TAR	Gore TAG	26/26/100

Notes. TEVAR: Thoracic endovascular aortic repair; MCA: motorcycle accident; CA: car accident; TAR: traumatic aortic rupture.

of the left ventricle was assessed by measuring the left E/E′ ratio (the ratio between early mitral inflow velocity and mitral annular early diastolic velocity) and E/A ratio (the ratio of peak velocity blood flow from gravity in early diastole to peak velocity flow in late diastole caused by atrial contraction).

Cardiovascular magnetic resonance protocol

All patients and healthy controls underwent a comprehensive, non-contrast cardiovascular magnetic resonance (CMR) study using a 1.5-T Siemens Aera scanner (Siemens Healthcare, Erlangen, Germany) between September 2019 and February 2020. This examination was performed in the Department of Electrophysiology, Heart Center, at the Technische Universität Dresden. Brachial systolic and diastolic pressures were measured immediately before the procedure.

The protocol included a stack of still 2D balanced steady-state free precession (bSSFP) images in the sagittal plane covering the whole aorta with vectorcardiogram (VCG) gating (end diastole), end-expiratory breath-hold, with repetition time (TR)=34.71, echo time (TE)=1.16 ms, flip angle (FA)=60°, slice thickness 5 mm, acquisition matrix 384×512, variable field of view (FOV), and in-plane resolution of 0.74×0.74 (Figure 1).

Cine bSSFP imaging was performed using breath-hold retrospective VCG gating to acquire a stack of short-axis slices and three long-axis views (two-, three-, and four-chamber), as shown in Figure 2. Short-axis images were acquired with a slice thickness of 8 mm (with a 2-mm gap), FA=60°, variable FOV, a 186×192 matrix, and a temporal resolution of 35–45 ms (with a reconstruction of 25 frames per RR interval). Long-axis images were acquired with a slice thickness of 6 mm, FA=60°, variable FOV, a 180×192 matrix, and a temporal resolution of 35–45 ms (with a reconstruction of 25 frames per RR interval). Parallel imaging-generalized auto-calibrating partially parallel acquisition (GRAPPA) was utilized with an acceleration factor of 2.
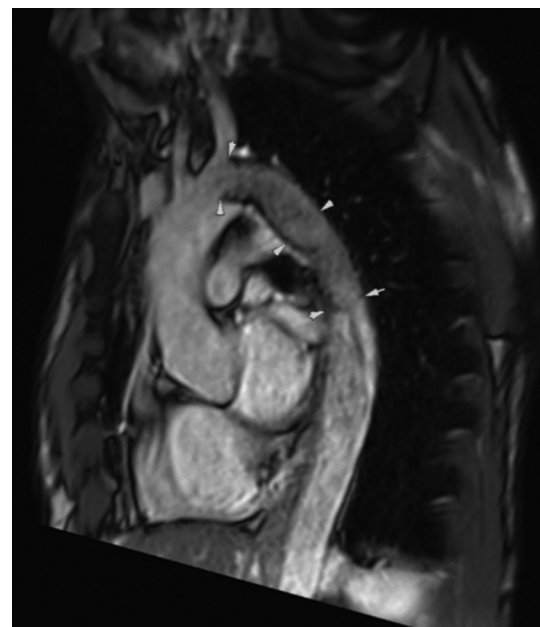

Figure 1. Cardiovascular magnetic resonance imaging (2D balanced steady-state free precession) showing the whole aorta and aortic stent placement in the sagittal plane. White arrows indicate the proximal, mid-portion, and distal ends of the stent. In this example, the bird-beak configuration of the proximal stent end after thoracic endovascular aortic repair (TEVAR) could be evaluated. AAo: ascending aorta; AAr: aortic arch; DAo: descending aorta; TAo: thoracic aorta.

T1-mapping was performed using shortened modified look-locker inversion recovery (ShMOLLI) collected using bSSFP readouts in a single breath-hold, TR=277.51 ms, TE=1.2 ms, FA=35°, matrix=154×192, interpolated pixel size=0.9×0.9 mm.

The 4D flow dataset covering the thoracic and partial abdominal aorta was acquired with retrospective VCG gating during free breathing (Figure 3). The sequence (WIP 785A) utilized 3D Cartesian sampling with flow encoding and GRAPPA acceleration, the reference lines were acquired separately (ePAT), and an acceleration factor of 2 was applied in both the phase-encoding and partition-encoding directions. Acquisition parameters (velocity encoding 200 cm/s, FOV 300×400 mm, matrix 77×160, FA=7°, TR=37.84 ms, TE=2.1) had been set to produce an
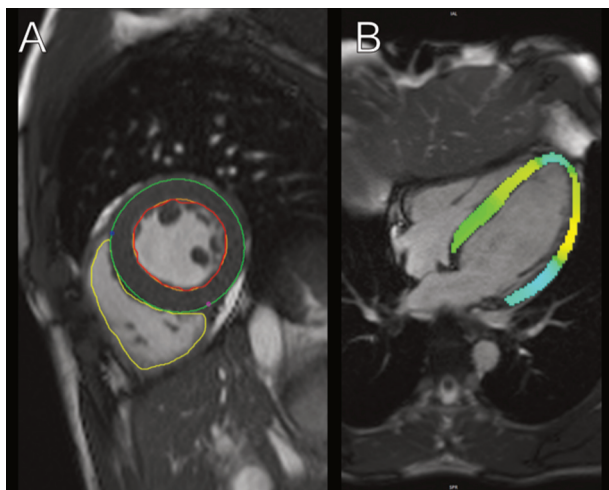
Figure 2. Cardiovascular magnetic resonance cine bSSFP imaging of the heart during breath-hold. Left picture (A) showing a short-axis view of the heart at a mid-ventricular level with automatic segmentation of the right ventricle (RV, yellow) and left ventricle (LV) with its endo- (orange) and epi-(green) myocardial boarders for quantification of cardiac volumes, function, myocardial mass and further indices. Right picture (B) showing a four-chamber long-axis view of the heart with automatic left ventricular (LV) myocardial strain analysis (cvi24, release 5.12.1, Circle Cardiovascular Imaging, Calgary, Canada). bSSFP: balanced steady-state free precession; RA: right atrium; LA: left atrium; Ao; aorta.

isotropic dataset with voxel size of 2.5×2.5×2.5 mm, acceptable signal-to-noise ratio. A total of 40 frames per RR interval were reconstructed, resulting in a calculated temporal resolution of 17–25 ms depending on the heart rate (60–90 bpm).

Offline image analysis

The diameters at the aortic annulus, aortic root (cusp-commissure), sinotubular junction, mid-ascending aorta, aortic arch, descending aorta distal to the left subclavian artery, and abdominal aorta at the level of the diaphragm were measured with multiplanar reconstruction (MPR) of the sagittal bSSFP image stack. Indexed diameters were calculated using the Mosteller formula.

The cine images were processed using automatic segmentation of the left ventricle (LV) and right ventricle (RV) blood-pool cavity and myocardium (cvi24, release 5.12.1, Circle Cardiovascular Imaging, Calgary, Canada; Figure 2). Nominal and indexed LV and RV end-systolic and end-diastolic volumes, as well as left ventricular myocardial mass and peak thickness at diastole, were determined. Left atrial (LA) volumes were estimated using two- and four-chamber long-axis views.

LV myocardial strain analysis was performed using automatically segmented lines (Figure 2), and LA strain analysis was performed after manually contouring the mitral valve annulus and LA endocardium.

The myocardial septal T1 values at the mid-ventricular level were measured in the short-axis images, and the regions of interest (ROI) were manually contoured in the ShMOLLI T1-maps.

Statistical analysis

Continuous data were reported as mean±standard deviation. In the case of outliers, the data were reported as median, 25%, and 75% quartiles. For between-group comparisons, the normality of the data was verified using box plots and the Kolmogorov–Smirnov normality test. Normally distributed data comparisons were performed using Student's t-test for independent groups. In cases where data were not normally distributed, the non-parametric Wilcoxon rank-sum test was used.

Categorical data were summarized as frequencies and percentages. Categorical data were compared using either Fisher's exact test or the Chi-square test, where applicable. The results were expressed in terms of p-values. Two-sided statistical significance was considered for a p-value <0.05.

Statistical analyses were performed using the STATA software version 13.1 (Stata Corp, College Station, TX, USA).

Results

Demographic data

Table I presents the results of the demographic data analysis. The analysis showed inconspicuous patient groups with
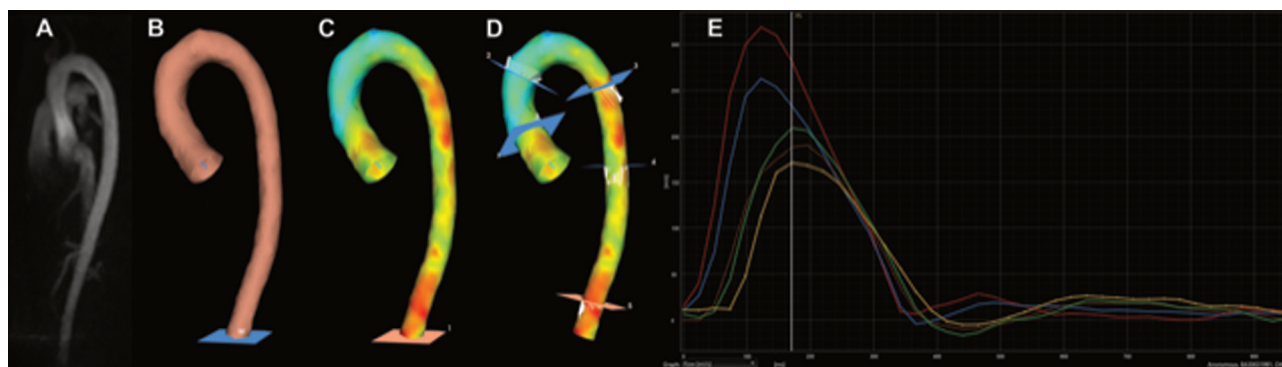

Figure 3. Example of 4D flow CMR imaging and post-processing of the whole aorta showing (A) angiographic reconstruction, (B) endovascular 3D model reconstruction, (C) with color-coded information of pulse wave velocities (PWV, low: blue/green; high: orange/red), (D) at different aortic levels of PWV measurement and their (E) time course over the cardiac cycle. CMR: cardiovascular magnetic resonance; PWV: pulse wave velocity.

Table III. Cardiac measurements

Variable	TEVAR group (N=10)	Healthy control group (N=10)	p-value
LVEF (%)	59.9±5.0	62.7±3.0	0.150
LVEDVI (ml/m^2)	84.8±16.1	82.1±9.6	0.647
RVEF (%)	57.3±7.0	57.7±3.8	0.859
RVEDVI (ml/m^2)	86.5±14.0	87.1±12.1	0.922
LAVI (ml/m^2)	39.2±11.5	34.6±9.1	0.335
E velocity (m/s)	0.39±0.09	0.39±0.09	0.967
A velocity (m/s)	0.26±0.07	0.19±0.06	0.012
E/A ratio	1.56±0.45	2.15±0.76	0.047
3D systolic LV-longitudinal strain (%)	12.13±2.31	13.20±1.96	0.279
3D diastolic LV-longitudinal strain rate (1/s)	0.70±0.17	0.89±0.18	0.026
3D diastolic LV-longitudinal vel. (m/s)	0.59±0.13	0.74±0.10	0.013

Notes. TEVAR: Thoracic Endovascular Aortic Repair; N: Number of Patients; LVEF: Left ventricular ejection fraction; LVEDVI: Left ventricular end diastolic volume index; RVEF: right ventricular ejection fraction; RVEDVI: right ventricular end diastolic volume index; LAVI: left atrial volume index; LV: left ventricle; E: E diastolic wave of pulsed wave doppler of the left ventricle; A: A diastolic wave of pulsed wave doppler of the left ventricle; vel: velocity.

Table IV. Aortic measurements

Variable	TEVAR group (n=10)	Healthy control group (N=10)	p-value
Aortic ring (mm/m^2)	13.7±1.4	12.9±1.3	0.165
Aortic root (mm/m^2)	16.8±1.8	15.4±2.0	0.117
Ascending aorta (mm/m^2)	16.1±2.0	13.5±1.9	0.007
Aortic arch (mm/m^2)	12.4±1.5	11.5±1.4	0.157
Descending aorta (mm/m^2)	12.0±1.4	11.6±1.7	0.544
Abdominal aorta (mm/m^2)	10.4±1.2	10.0±1.3	0.441
PWV global oscillometry (m/s)	9.8 [8.4, 12.2]	7.0 [6.2, 8.2]	0.001
PWV global 4D flow (m/s)	5.9 [5.7, 6.7]	4.8 [4.5, 6.0]	0.012
PWV ascending aorta 4D flow (m/s)	5.9 [4.8, 6.8]	5.3 [4.4, 6.4]	0.504
PWV aortic arch 4D flow (m/s)	3.6 [2.8, 4.4]	3.4 [3.2, 3.9]	0.894
PWV descending aorta 4D Flow (m/s)	19.1 [8.4, 24.0]	6.2 [5.2, 7.4]	0.003
PWV abdominal aorta 4D flow (m/s)	8.7 [6.4, 10.2]	6.6 [5.8, 6.8]	0.032

Notes. TEVAR: thoracic endovascular aortic repair; PWV: pulse wave velocity.

no significant difference between the two groups, with a mean age of 36 years, a mean body surface area of 2.0 m^2, and two female patients in each group. The mean age of the patients in the TEVAR group at the time of thoracic endovascular aortic repair (TEVAR) was 30 years.

Cardiac measurements

The mean diastolic wall thickness index was significantly higher in the TEVAR group than in the control group (11.7±1.2 mm vs. 9.7±0.9; p=<0.001). The right and left ejection fractions, right and left ventricular volume indices, and left atrial volume index were not significantly different between the groups (Table III). Furthermore, pulsed wave Doppler showed a higher A wave and a lower E/A ratio in the TEVAR group than in the control group (Table II). The 3D systolic left ventricular longitudinal strain did not differ significantly between the groups. The 3D diastolic left ventricular strain rate and velocity were lower in the TEVAR group than in the control group (Table III). Native T1 results were significantly higher in the TEVAR group

compared with those in the control group (1007.8±26.7 vs. 982.1±24.6 ms, p=0.037).

Aortic measurements

The static measurement of the aorta showed a larger ascending aorta diameter in the TEVAR group compared with that in the control group (16.1±2.0 mm/m^2 vs. 13.5±1.9 mm/m^2; p=0.007). The diameters of the aortic annulus, root, and arch, descending thoracic aorta, and abdominal aorta were not significantly different between the groups (Table IV).

4D flow measurements

The median global 4D flow pulse wave velocity (PWV) was significantly higher in the TEVAR group than in the control group (5.9 [5.7, 6.7] vs. 4.8 [4.5, 6.0] m/s; p=0.012). The regional 4D flow analysis showed a higher PWV in the TEVAR group than in the control group distal to the aortic stent position, with a PWV of 19.1 [8.4, 24.0] vs.
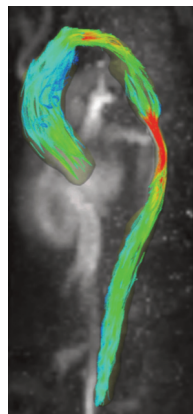
Figure 4. 4D flow cardiovascular magnetic resonance (CMR) assessment and reconstruction along the aorta and the stent in a TEVAR patient. Blood flow pattern are visualised using systolic streamlines. The color-coding indicates speed of blood flow from low (green) to high (red) especially at the proximal end of the stent and even more impressive at the distal end of the stent. Concordant to this finding, elevated wall sheer stress (red color) in the thoracic aorta right after the distal end of the stent can be measured. TEVAR: thoracic endovascular aortic repair.

6.2 [5.2, 7.4] m/s in the descending thoracic aorta and 8.7 [6.4, 10.2] vs. 6.6 [5.8, 6.8] m/s in the abdominal aorta, respectively (p=0.003 and 0.032, respectively; Figure 4). The analysis showed no significant differences between the groups in the 4D flow PWV proximal to the aortic stent (i.e., in the ascending aorta and aortic arch). Table III presents the results.

Discussion

Blunt thoracic aortic injury (BTAI) is a life-threatening condition, and thoracic endovascular aortic repair (TEVAR) has proven to be an effective therapy with high efficiency and low perioperative risk compared with open surgery [1]. As a high percentage of patients undergoing TEVAR for BTAI are young, the long-term effect of TEVAR on the cardiovascular system is gaining more attention.

Kadoglou et al. reported that TEVAR is associated with increased aortic stiffness [3], which might, in turn, affect cardiac performance and proximal aortic segments. Sultan et al. described several cases with developed ventricular hypertrophy with diastolic dysfunction within 2 years after TEVAR and following endovascular aortic repair (EVAR) [5].

An increase in arterial stiffness can have a detrimental effect on cardiac performance through two mechanisms: an increase in afterload in systole and a decrease in coronary perfusion in diastole. Physiologically, the antegrade pulse wave (i.e., from the heart to the periphery) that originates during systole with myocardial contraction and the flow of blood into the aorta is reflected back (i.e., from the periphery to the heart) at the point of sudden increase in arterial resistance (e.g., at the point of arterial branching) [6]. An increase in arterial stiffness leads to an increase in the pulse wave velocity (PWV). With the increase in PWV,

the reflected pulse starts earlier than expected and is reflected back toward the heart within the systolic phase, increasing the afterload and cardiac work in systole. During diastole, an increase in arterial stiffness leads to a decrease in Windkessel function. The elastic aorta stores up to 50% of the left ventricular stroke work during systole. Owing to its elasticity, it regains its smaller diameter in diastole, releasing the stored energy and maintaining the perfusion pressure in diastole [7, 8]. As most cardiac perfusion occurs during diastole, a decrease in the Windkessel effect negatively affects cardiac perfusion [5]. This means that with increased arterial stiffness, the systolic workload of the heart increases, while its perfusion decreases [9]. Although the presented analysis of cardiac measurements did not have a significant ischemic consequence, with no significant difference in longitudinal systolic strain, it showed a significant increase in myocardial wall thickness with subsequent diastolic dysfunction, as confirmed by the significant increase in diastolic strain rate and velocity in the TEVAR group. This shows the effect of increased afterload after TEVAR due to increased wall stiffness and indicates the need for a systematic long-term follow-up of cardiac performance after TEVAR. Clinically, these pathologic changes might have led to the development of manifest arterial hypertension in the four TEVAR patients, who required permanent antihypertensive drug therapy at an early age.

The increase in wall stiffness not only affects myocardial performance, but also affects the proximal aorta itself. The increase in pulse pressure, which results from increased stiffness, is one of the main causes of large-artery degeneration and elastin fiber fatigue and fracture [10]. This leads to a decrease in wall elasticity and development of aneurysms [11]. The analysis of cardiovascular magnetic resonance (CMR) measurements in our study confirmed a significant increase in ascending aorta diameter in the TEVAR group. This requires special attention in future research by studying the biomechanical and long-term histochemical effects of TEVAR on the proximal aorta and development of proximal aortic pathology in this cohort of patients. The review article of Sultan et al. summarises the known negative effects after TEVAR and EVAR on cardiovascular hemodynamic changes and major adverse clinical outcome and emphasizes that a 4-dimensional strategy in managing patients with complex aortic pathologies and treatment with stent-graft materials is necessary [12].

As this study shows the importance of long-term vascular and cardiac follow-up after TEVAR for BTAI, a comprehensive radiation-free evaluation by CMR serves as an excellent single investigation method that increases in value to achieve both goals in patients with a repetitive need for aortic and cardiac imaging. Voges et al. reported normal PWV values in young adults using CMR [13]. This was followed by Harloff et al., who used 4D flow magnetic resonance imaging (MRI) to assess aortic stiffness accurately [14]. CMR can also be used to adequately measure cardiac performance including myocardial strain [15, 16]. Although previously not recommended as a standard imaging

technique for evaluating cardiovascular risk in asymptomatic patients owing to its high cost [17], we believe that the use of CMR for cardiac and vascular evaluation in this specific cohort of patients is required and should be implemented.

As the results of this study highlight the effect of aortic stiffness on myocardial performance and proximal vascular structures, we believe that more attention should be provided to the design and materials used for stent manufacturing. Kadoglou et al. reported a higher PWV and arterial stiffness in patients receiving polyester-covered stent–grafts than in those receiving polytetrafluoroethylene (PTFE)-covered stent–grafts [3]. Further studies and collaboration with the industry are needed to improve the stent–graft design and material to achieve optimum endovascular therapy while alleviating the long-term effects on the cardiovascular system.

Limitations

This case-controlled study investigated a small sample size of selected patients using a retrospective design. This may have affected the generalisability of our results. Further multicentre studies or registries with a larger cohort and precise algorithm for examination of PWV, echocardiography, and CMR are needed to further investigate cardiovascular complications following TEVAR for BTAI.

Conclusions

Young patients with blunt injury of the thoracic aorta (BTAI) appear to be at increased risk of developing vascular dysfunction with secondary myocardial diastolic dysfunction due to increased aortic stiffness following thoracic endovascular aortic repair (TEVAR). Patients with BTAI therefore require follow-up for detection adverse and/or cardiac developments and complications in follow-up. In addition to depicting vascular anatomy, cardiovascular magnetic resonance (CMR) allows for comprehensive and radiation-free evaluation of vascular stiffness and associated myocardial changes at early and subclinical stages.

References

1. Lee WA, Matsumura JS, Mitchell RS, Farber MA, Greenberg RK, Azizzadeh A, et al. Endovascular repair of traumatic thoracic aortic injury: clinical practice guidelines of the Society for Vascular Surgery. J Vasc Surg. 2011;53:187–92. https://doi.org/10.1016/j.jvs.2010.08.027
2. Upchurch GR, Escobar GA, Azizzadeh A, Beck AW, Conrad MF, Matsumura JS, et al. Society for Vascular Surgery clinical practice guidelines of thoracic endovascular aortic repair for descending thoracic aortic aneurysms. J Vasc Surg. 2021; 73(1):55S–83S. https://doi.org/10.1016/J.JVS.2020.05.076
3. Kadoglou NP, Moulakakis KG, Papadakis I, Ikonomidis I, Alepaki M, Spathis A, et al. Differential effects of stent-graft fabrics on arterial stiffness in patients undergoing endovascular aneurysm repair. J Endovasc Ther. 2014;21:850–8. https://doi.org/10.1583/14-4772MR.1
4. Mitchell RS, Ishimaru S, Ehrlich MP, Iwase T, Lauterjung L, Shimono T, et al. First International Summit on Thoracic Aortic Endografting: roundtable on thoracic aortic dissection as an indication for endografting. J Endovasc Ther. 2002;9(Suppl 2):98–105.
5. Sultan S, Acharya Y, Hazima M, Salahat H, Parodi JC, Hynes N. Combined thoracic endovascular aortic repair and endovascular aneurysm repair and the long-term consequences of altered cardiovascular haemodynamics on morbidity and mortality: case series and literature review. Eur Heart J Case Rep. 2021;5(10):ytab339.
6. Tomiyama H, Yamashina A. Non-invasive vascular function tests: their pathophysiological background and clinical application. Circ J. 2010;74(1):24–33. https://doi.org/10.1253/CIRCJ.CJ-09-0534
7. Nauta FJH, de Beaufort HWL, Conti M, Marconi S, Kamman AV, Ferrara A, et al. Impact of thoracic endovascular aortic repair on radial strain in an ex vivo porcine model. Eur J Cardiothorac Surg. 2017;51(4):783–9. https://doi.org/10.1093/EJCTS/EZW393
8. Belz GG. Elastic properties and of the human aorta windkessel function. Cardiovasc Drugs Ther. 1995;9(1):73–83.
9. Mandigers TJ, Bissacco D, Domanin M, Piffaretti G, van Herwaarden JA, Trimarchi S. Complications and failure modes in the proximal thoracic aorta the pros and cons of management options for aortic pathology, including branched TEVAR. 2021;20(11):60–4.
10. O'Rourke MF, Hashimoto J. Mechanical factors in arterial aging: a clinical perspective. J Am Coll Cardiol. 2007;50(1):1–13. https://doi.org/10.1016/j.jacc.2006.12.050
11. Jana S, Hu M, Shen M, Kassiri Z. Extracellular matrix, regional heterogeneity of the aorta, and aortic aneurysm. Exp Mol Med. 2019;51(12):1–15. https://doi.org/10.1038/s12276-019-0286-3
12. Sultan S, Acharya Y, Soliman O, Parodi JC, Hynes N. TEVAR and EVAR, the unknown knowns of the cardiovascular hemodynamics; and the immediate and long-term consequences of fabric material on major adverse clinical outcome. Front Surg. 2022;9:940304. https://doi.org/10.3389/fsurg.2022.940304
13. Voges I, Jerosch-Herold M, Hedderich J, Pardun E, Hart C, Gabbert DD, et al. Normal values of aortic dimensions, distensibility, and pulse wave velocity in children and young adults: a cross-sectional study. J Cardiovasc Magn Reson. 2012;14(1):77. https://doi.org/10.1186/1532-429X-14-77v
14. Harloff A, Mirzaee H, Lodemann T, Hagenlocher P, Wehrum T, Stuplich J, et al. Determination of aortic stiffness using 4D flow cardiovascular magnetic resonance-a population-based study. J Cardiovasc Magn Reson. 2018;20(1):43. https://doi.org/10.1186/s12968-018-0461-z
15. Leiner T, Bogaert J, Friedrich MG, Mohiaddin R, Muthurangu V, Myerson S, et al. SCMR Position Paper (2020) on clinical indications for cardiovascular magnetic resonance. J Cardiovasc Magn Reason. 2020;22(1):76. https://doi.org/10.1186/S12968-020-00682-4
16. Scatteia A, Baritussio A, Bucciarelli-Ducci C. Strain imaging using cardiac magnetic resonance. Heart Fail Rev. 2017;22(4):465–76. https://doi.org/10.1007/s10741-017-9621-8
17. Greenland P, Alpert JS, Beller GA, Benjamin EJ, Budoff MJ, Fayad ZA, et al. 2010 ACCF/AHA guideline for assessment of cardiovascular risk in asymptomatic adults. J Am Coll Cardiol. 2010;56(25):e50–103. https://doi.org/10.1016/J.JACC.2010.09.001

ORCID
Tamer Ghazy
 https://orcid.org/0000-0003-2413-4065
Jakub Tomala
 https://orcid.org/0000-0001-6823-678X
Igli Kalaja
 https://orcid.org/0000-0003-1082-5578
Marc Irqsusi
 https://orcid.org/0000-0003-1422-2889

Ardawan Rastan
 https://orcid.org/0000-0002-2400-5098
Helmut Karl Lackner
 https://orcid.org/0000-0002-0159-3720

Correspondence address
PD Dr. med. Adrian Mahlmann
Kath. Krankenhaus Hagen gGmbH
Dreieckstr. 17
58097 Hagen
Germany

mahlmanna@kkh-hagen.de